

Universality of stochastic control of quantum chaos with measurement and feedback

Andrew A. Allocca,^{1,2} Devesh K. Verma,¹ Sriram Ganeshan,^{3,4} and Justin H. Wilson^{1,2}

¹*Department of Physics and Astronomy, Louisiana State University, Baton Rouge, Louisiana 70803, USA*

²*Center for Computation and Technology, Louisiana State University, Baton Rouge, Louisiana 70803, USA*

³*Department of Physics, City College, City University of New York, New York 10031, USA*

⁴*CUNY Graduate Center, New York, New York 10031, USA*

We investigate quantum dynamics in the vicinity of an unstable fixed point subjected to stochastic control. The stochastic competition between the system's inherent instability (pushing trajectories away) and engineered control dynamics (drawing them back to the same point) forms the core of probabilistic control in chaotic systems. Recent studies reveal that this interplay underlies a family of measurement- and feedback-driven dynamical quantum phase transitions. To capture its universal features, we consider the inverted harmonic oscillator, a canonical model whose operator amplitudes diverge. Our control scheme, a quantum version of classical attractor dynamics, employs non-unitary evolution via measurements and conditional resets. By combining numerical simulations, a semiclassical Fokker–Planck analysis, and direct spectra of the quantum channel, we map out the control transition and uncover quantum-specific signatures of the underlying dynamics. We demonstrate the universality of our results within the quantum Arnold cat map, a paradigmatic model of quantum chaos.

Introduction—Order emerges from chaotic dynamics across a range of scales, from microscopic quantum systems to macroscopic classical, and even socio-economic, processes. In many-body systems, local interactions are sufficient to induce ordering. Bird flocks and fish schools provide familiar classical examples [1, 2], superconductivity and superfluidity represent analogous quantum phenomena, and within statistical mechanics, ordered states emerge through phase transitions.

Beyond passive emergence, order can be engineered from chaotic dynamics using both deterministic procedures, e.g. the Ott–Grebogi–Yorke method [3], and probabilistic approaches, involving the stochastic intervention of a control map with probability p into chaotic dynamics [4–6]. The control map and chaotic dynamics share a periodic orbit, unstable for the latter and stable for the former, which becomes a global attractor above a critical control rate p_c . This is a random multiplicative process where distance from the control point $\delta\mathbf{r}$ is either amplified by a factor e^κ by chaotic dynamics or contracted by a factor $e^{-\gamma}$ by control; this has been studied in turbulent systems [7–10] and market dynamics [11–18]. These ideas have also recently gained resonance in quantum systems, where measurement-conditioned feedback operations can stabilize states and steer dynamics [19–31].

In this Letter, we investigate the stochastic control of quantum systems onto unstable *classical* periodic orbits of discrete (Floquet) dynamics with unitary quantizations. Near these orbits, the problem reduces to the inverted harmonic oscillator (IHO) [32] due to the classical phase space being of even dimension with a symplectic structure, i.e. a Poisson bracket. Additionally, the system has quantum fluctuations described by the uncertainty principle. Implementing stochastic control quantum mechanically involves a nonunitary process, i.e. measurement and feedback, since unitarity can-

not favor one state. While the IHO omits rich dynamics in the uncontrolled phase—such as self-interference and entanglement—it enables us to capture the control transition and controlled phase.

We begin with the classical stochastic control problem and its known features, then introduce the quantum control problem, which involves a non-unitary channel enriched by quantum fluctuations. By numerically solving the random Gaussian state dynamics, we establish random-walk universality and make this connection explicit with a Fokker–Planck (FP) analysis. For the non-Gaussian full channel, we find eigenoperators of the evolution which are related to moments of quantum operators and are only finite for $p > p_n^* > p_c$ (for the n th moment), matching FP in its regime of applicability. Finally, we show how this transition is a crossover in the quantization of the Arnold cat map, but becomes exact in the $\hbar \rightarrow 0$ limit. In all, we obtain the critical point p_c , critical scaling near the transition, and the complete statistical distribution including operator moments.

Classical Control—Take $\delta\mathbf{r}(t)$ to be the displacement in 2d phase space from an unstable fixed point or periodic orbit with discrete time index t . The chaotic and control maps act on $\delta\mathbf{r}(t)$ as $\mathcal{S} = \text{diag}(e^\kappa, e^{-\kappa})$ and $\mathcal{C} = \text{diag}(e^{-\gamma}, e^{-\gamma})$ respectively, with $\kappa, \gamma > 0$ parameterizing their respective strengths ($\det \mathcal{S} = 1$ due to being area-preserving). The behavior of the first component δr_1 determines controllability of the system: chaos is controlled when $\ln |\overline{\delta r_1(t)}| < 0$ as $t \rightarrow \infty$, where $\overline{(\cdots)}$ represents averaging over stochastic trajectories. The average of this quantity can be performed analytically, resulting in a critical control rate [6, 33],

$$p_c = \frac{\kappa}{\kappa + \gamma}, \quad (1)$$

above which the system is controlled, and below which chaos prevails.

Quantum Model—We obtain a quantum model by promoting the two phase space dimensions to canonical operators \hat{x} and \hat{p} with $[\hat{x}, \hat{p}] = i$ with $\hbar = 1$. The IHO captures the saddle-point structure near an unstable fixed point,

$$\hat{H} = \frac{\hat{p}^2}{2} - \frac{\Omega^2 \hat{x}^2}{2}, \quad (2)$$

where Ω controls the strength of the potential. Time evolution under this Hamiltonian generates a single-mode squeezing operation $\hat{U}(t) = \exp(-i\hat{H}t)$ and a Heisenberg-picture quantum channel

$$\mathbb{S}[\hat{O}] = \hat{U}^\dagger(t) \hat{O} \hat{U}(t). \quad (3)$$

The action of this channel for time t_S models a “quantum-chaotic” map, and $\kappa \equiv \Omega t_S$ characterizes its strength. The operators $\hat{v}_\pm \equiv \sqrt{\Omega/2}(\hat{x} \pm \hat{p}/\Omega)$ grow or decay, $\mathbb{S}[\langle \hat{v}_\pm \rangle] = e^{\pm\kappa} \langle \hat{v}_\pm \rangle$, so these and their powers and products are eigenvectors of this channel; $\langle \hat{v}_\pm \rangle$ are analogs of the components of $\delta \mathbf{r}$ above.

We can define ladder operators \hat{a} , \hat{a}^\dagger , and the associated number states $|n\rangle$ as for the normal harmonic oscillator. The vacuum $|0\rangle$ is an unstable fixed point of IHO evolution, and is our target for control, which is implemented with weak measurements. We introduce an ancilla mode with ladder operators \hat{b} , \hat{b}^\dagger and number states $|n\rangle_b$, initialized in $|0\rangle_b$, and couple this to the original system via the Hamiltonian $\hat{H}_{\text{ctrl}} = J(\hat{a}^\dagger \hat{b} + \hat{a} \hat{b}^\dagger)$ with coupling strength J . By evolving the combined system with \hat{H}_{ctrl} for time t_C , then measuring the ancilla in the number basis and resetting it to $|0\rangle_b$, the main system is pushed towards $|0\rangle$. The Kraus operators for this operation are,

$$\begin{aligned} \hat{K}_m(\theta) &= \langle m |_b e^{-iJt_C(\hat{a}^\dagger \hat{b} + \hat{a} \hat{b}^\dagger)} |0\rangle_b \\ &= \frac{(-i)^m}{\sqrt{m!}} \sin^m(\theta) (\cos(\theta))^{\hat{a}^\dagger \hat{a}} \hat{a}^m, \end{aligned} \quad (4)$$

where $\theta \equiv Jt_C$ and m is the outcome of the measurement on the ancilla. The corresponding quantum channel acts on operators as

$$\mathbb{C}[\hat{O}] = \sum_{m=0}^{\infty} \hat{K}_m^\dagger(\theta) \hat{O} \hat{K}_m(\theta). \quad (5)$$

For any linear combination of canonical operators, e.g. \hat{x} , \hat{p} , \hat{v}_\pm , the action of \mathbb{C} is multiplication by $\cos\theta$, so putting $\cos\theta = e^{-\gamma}$ this channel acts as the classical control map. Furthermore, all normally-ordered products of \hat{a} and \hat{a}^\dagger are eigenvectors of this channel, $\mathbb{C}[(\hat{a}^\dagger)^k \hat{a}^l] = \cos^{k+l}(\theta) (\hat{a}^\dagger)^k \hat{a}^l$.

The full stochastic evolution of a generic operator is the weighted sum of these two channels

$$\hat{O}(t+1) = \mathbb{T}[\hat{O}(t)] = (1-p)\mathbb{S}_\kappa[\hat{O}(t)] + p\mathbb{C}_\gamma[\hat{O}(t)], \quad (6)$$

where we have labeled the channels by their respective exponential parameters.

Quantum dynamics and Gaussian state evolution—The dynamics of $\langle \hat{v}_\pm \rangle$ under \mathbb{S}_κ and \mathbb{C}_γ follow the classical dynamics, so classical arguments suffice to understand control of linear operators. To observe quantum effects beyond the classical limit, we must look to higher orders in canonical operators. The covariance matrix,

$$\sigma_{ij} = \frac{1}{2} \langle \{\hat{r}_i, \hat{r}_j\} \rangle - \langle \hat{r}_i \rangle \langle \hat{r}_j \rangle \quad (7)$$

where $\hat{\mathbf{r}} = (\hat{v}_+, \hat{v}_-)^T$ and $\{\cdot, \cdot\}$ is the anticommutator, contains all Gaussian operators, and along with $\langle \hat{\mathbf{r}} \rangle$ it characterizes Gaussian states. To highlight the quantum aspects of control we take $\langle \hat{\mathbf{r}} \rangle = 0$, so the system is always controlled from the classical perspective. Evolution of σ under \mathbb{S}_κ and \mathbb{C}_γ is

$$\mathbb{S}_\kappa[\sigma] = \begin{pmatrix} e^{2\kappa}\sigma_{11} & \sigma_{12} \\ \sigma_{12} & e^{-2\kappa}\sigma_{22} \end{pmatrix} \quad (8)$$

$$\mathbb{C}_\gamma[\sigma] = e^{-2\gamma} \sigma + \frac{1}{2} (1 - e^{-2\gamma}) \mathbf{1}. \quad (9)$$

By design \mathbb{S}_κ is a single-mode squeezing channel, and \mathbb{C}_γ is a pure-loss attenuator [34]. For $p \neq 0$ the off-diagonal elements of σ are only affected by control and vanish for $t \rightarrow \infty$, so only $\sigma_{11}, \sigma_{22} \equiv \sigma_\pm$ are relevant for steady state properties. These are proportional to the uncertainties of canonical variables, and the constant term in \mathbb{C}_γ manifests the quantum uncertainty relation ensuring that $\sigma_+ \sigma_- \geq 1/4$; its fixed point is $\sigma_\pm = 1/2$. The action of \mathbb{S}_κ and \mathbb{C}_γ on σ_\pm do not commute, complicating the general analysis of the trajectories of σ_\pm , however the system can be analyzed numerically together with analytical methods applicable in particular limits.

Semiclassical analysis of quantum control transition—Because $|0\rangle$ is the target state, the late-time trajectory-averaged fidelity with $|0\rangle$, i.e. $\bar{\rho}_{00} \equiv \langle 0 | \rho(t \rightarrow \infty) | 0 \rangle$, is an order parameter for control, where $\rho(t)$ is the density matrix at time step t . The controlled state is signaled by $\bar{\rho}_{00} > 0$. Because both \mathbb{S}_κ and \mathbb{C}_γ are Gaussian channels, trajectories initialized in a Gaussian state remain Gaussian. With our assumption $\langle \hat{\mathbf{r}} \rangle = 0$, $\rho_{00}(t)$ for a Gaussian trajectory is [34]

$$\rho_{00}(t) = \frac{1}{\sqrt{(\sigma_+(t) + \frac{1}{2})(\sigma_-(t) + \frac{1}{2})}}. \quad (10)$$

Since an arbitrary density matrix can be written as a linear combination of Gaussian density matrices, the order parameter $\bar{\rho}_{00}$ capturing the behavior of a generic state is

$$\bar{\rho}_{00} = \int d\sigma_+ d\sigma_- \frac{\mathcal{Q}(\sigma_+, \sigma_-)}{\sqrt{(\sigma_+ + \frac{1}{2})(\sigma_- + \frac{1}{2})}}, \quad (11)$$

where $\mathcal{Q}(\sigma_+, \sigma_-)$ is the steady-state probability density over Gaussian trajectories which obeys

$$\mathcal{Q}(\sigma_+, \sigma_-) = (1-p)\mathcal{Q}(\mathbb{S}_\kappa^{-1}[\sigma_+, \sigma_-]) + p\mathcal{Q}(\mathbb{C}_\gamma^{-1}[\sigma_+, \sigma_-]). \quad (12)$$

This is analogous to the Frobenius-Perron equation for the invariant density used in classical chaotic dynamics [35] [36].

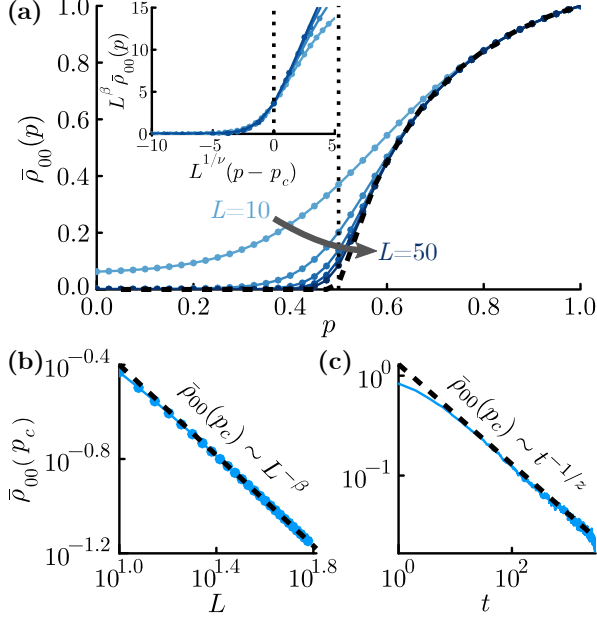


FIG. 1. (a) Steady-state $\bar{\rho}_{00}(p)$ computed as the fixed-point of \mathbb{T} using $\kappa = \gamma = 2 \ln \left(\frac{1+\sqrt{5}}{2} \right) \approx 0.42$ with $2^{-L-1} < \sigma_{\pm} < 2^{L-1}$ for $L = 10, 20, 30, 40, 50$. The black dashed line shows $\bar{\rho}_{00}$ obtained as the late-time average of 5000 random trajectories. The inset shows collapse near $p = p_c$ with $\nu = 1$ and $\beta = 0.96$. (b) Log-log plot of the steady-state values of $\bar{\rho}_{00}$ as a function of L at p_c , where $2^{-L-1} < \sigma_{\pm} < 2^{L-1}$. The black dashed line is $\bar{\rho}_{00} \propto L^{-\beta}$ with $\beta = 0.96$. (c) Log-log plot of the time dependence of $\bar{\rho}_{00}$ at p_c . The black dashed line is $\bar{\rho}_{00} \propto t^{-1/z}$ with $z = 2$.

In Fig. 1(a) we show $\bar{\rho}_{00}$ computed numerically as a late-time average over trajectories and as the fixed-point of the quantum channel, which necessitates implementing cutoffs $\sigma_+ \in (1/2, 2^{L-1})$ and $\sigma_- \in (2^{-L-1}, 1/2)$ —the action of \mathbb{S}_κ and \mathbb{C}_γ ensure that $0 < \sigma_- \leq 1/2$ and $\sigma_+ \geq 1/2$ for all p at late times. The two methods agree in the limit of large L , with convergence in the controlled phase since values of σ_{\pm} far from the control point are rarely explored. Despite considering only classically controlled states $\langle \hat{\mathbf{r}} \rangle = 0$ we find a clear control transition at p_c . Critical properties at p_c are obtained by examining how $\bar{\rho}_{00}$ varies with the cutoff L and in time, shown in Fig. 1(b,c), and by collapsing the p -dependence near $p = p_c$. Altogether, we find order parameter scaling exponent $\beta \approx 1$, dynamical exponent $z \approx 2$, and correlation length exponent $\nu \approx 1$, all characteristic of random walk universality.

Fokker-Planck analysis—Since $\sigma_- \in (0, 1/2)$ at late times, $\bar{\rho}_{00}$ vanishing or remaining nonzero must result from different behavior of σ_+ on either side of p_c : average σ_+ diverges for $p < p_c$, and remains finite for $p > p_c$.

By examining the stochastic dynamics of σ_+ as a random multiplicative process with lower bound $\sigma_+ > 1/2$ [37], we can capture many key qualitative features of the control transition. Consider the random process $\sigma_+(t+1) = \Lambda_t \sigma_+(t)$ where Λ_t is drawn randomly from $(e^{2\kappa}, e^{-2\gamma})$ with corresponding probabilities $(1-p, p)$, and with the constraint $\sigma_+ > 1/2$ imposed by hand. Transforming to $y = \ln \sigma_+$, in the limit of weak dynamics, i.e. κ, γ small, we can derive a FP equation for the distribution $P(y, t)$ of values taken by y during these dynamics,

$$\frac{\partial P(y, t)}{\partial t} = -\bar{v} \frac{\partial P(y, t)}{\partial y} + \mathcal{D} \frac{\partial^2 P(y, t)}{\partial y^2}, \quad (13)$$

with drift velocity and diffusion constant $\bar{v} = 2\kappa(p_c - p)/p_c$ and $\mathcal{D} = 2\kappa^2 p(1-p)/p_c^2$ respectively. This equation can be solved for both $P(y, t)$ away from the boundary at $y^{\min} = -\ln 2$ and for the nontrivial steady state distribution $P(y)$ for $p > p_c$,

$$P(y, t) \sim \frac{1}{\sqrt{2\pi\mathcal{D}t}} e^{-\frac{(y - \bar{v}t)^2}{2\mathcal{D}t}} \quad (14)$$

$$P(y) = \frac{\xi}{2\xi} e^{-\xi y} \Rightarrow \mathcal{Q}_+(\sigma_+) = \frac{\xi}{2\xi} \sigma_+^{-1-\xi}, \quad p > p_c, \quad (15)$$

where $\xi = |\bar{v}|/\mathcal{D}$. The distributions for σ_+ are obtained as $\mathcal{Q}_+(\sigma_+) = P(\ln \sigma_+)/\sigma_+$, and have log-normal and power-law forms respectively [38].

In Fig. 2, we compare the power-law form of $\mathcal{Q}_+(\sigma_+)$ to the distribution computed numerically for $p > p_c$. The lower boundary is vital for the existence of a late-time steady state—in Eq. (13) $\bar{v} < 0$ for $p > p_c$, so the distribution drifts to small y and is held up by the barrier at y^{\min} . These two opposing forces balance to yield a stable distribution. In the Supplement we also demonstrate log-normal behavior of $\mathcal{Q}_+(\sigma_+, t)$ at early times [39].

With solutions for the distribution we can examine critical behavior of the transition. At $p = p_c$, $\bar{v} = 0$ so the distribution has no overall drift and y evolves diffusively away from the boundary, yielding a divergence in y (and σ_+) at late times. Therefore the system evolves at late time as

$$\bar{\rho}_{00}(t) \sim \int_{\frac{1}{2}}^{\infty} d\sigma_+ \frac{\mathcal{Q}_+(\sigma_+, t)}{\sqrt{\sigma_+(t)}} \sim \int_0^{\infty} dy \frac{e^{-\frac{y^2}{2\mathcal{D}t}}}{\sqrt{\mathcal{D}t}} e^{-\frac{y}{2}} \sim t^{-1/2}. \quad (16)$$

If we now also impose a maximum $\sigma_+^{\max} = 2^L$, giving $y^{\max} = L \ln 2$, then for late times and large L the hard wall boundaries combined with the diffusive nature of P give $P(y) \sim 1/L$ and we have

$$\bar{\rho}_{00}(L) \sim \int_{\frac{1}{2}}^{2^L} d\sigma_+ \frac{\mathcal{Q}_+(\sigma_+)}{\sqrt{\sigma_+}} \sim \int_0^{L \ln 2} dy \frac{e^{-\frac{y}{2}}}{L} \sim \frac{1}{L}. \quad (17)$$

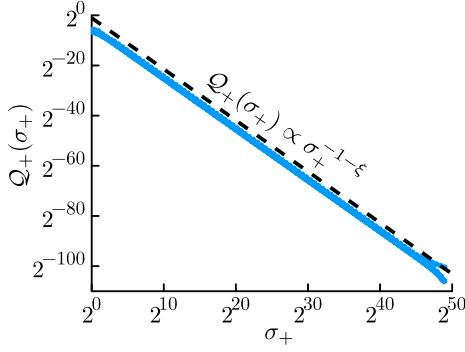


FIG. 2. Comparison of the power-law form of the distribution $Q_+(\sigma_+)$ acquired from the FP analysis with the distribution of σ_+ computed numerically from the fixed point of \mathbb{T} with $\kappa = \gamma = 0.2$ and cutoff $L = 50$ for $p = 0.6$.

The Fokker-Planck analysis therefore recovers the critical behavior observed numerically in Fig. 1(b,c) with exponents $\beta = 1$ and $z = 2$.

We can also examine the controllability of moments of this distribution. The late-time steady state distribution has power-law form, so each moment becomes finite at a higher control rate than guarantees normalizability:

$$\overline{\sigma_+^n} = \int d\sigma_+ \sigma_+^n Q_+(\sigma_+) = \frac{2^{-\xi} \xi}{\xi - n} \quad (18)$$

for $\xi > n$ and infinity otherwise. Setting $\xi = n$ gives a sequence of control rates at which moments of Q_+ can be controlled in the FP framework,

$$p_{2n}^{\text{FP}} = p_c + (1 - p_c)n\kappa + O(\kappa^2) > p_c, \quad (19)$$

where we have expanded the result in small κ since this was necessary to obtain Eq. (13) and $Q_+(\sigma_+)$. The n th moment of Q_+ is related to quantum operators of order $2n$ since σ_+ is quadratic.

Note that the multiplicative dynamics used to obtain Eq. (13) are only approximate. The map \mathbb{C}_γ imposes the constraint $\sigma_+ > 1/2$ in a smooth way, while our analysis here imposed it crudely, with the difference largest for $\sigma_+ \sim 1/2$. However, our results are controlled by the large- σ_+ properties of the distributions obtained from Eq. (13)—diffusive behavior away from the boundary and normalizability of distributions. The lower bound is essential for the existence of stable distributions, but features such as critical properties are insensitive to behavior near $\sigma_+ \sim 1/2$. We show this in the Supplement [39], where we derive a FP equation from the exact forms of \mathbb{S}_κ and \mathbb{C}_γ .

Exact quantum dynamics—The FP analysis developed above is semiclassical. We now obtain exact quantum results by constructing a set of eigenvectors \hat{Z}_n and corresponding eigenvalues λ_n for the full quantum channel \mathbb{T} , i.e. $\mathbb{T}[\hat{Z}_n] = \lambda_n \hat{Z}_n$. First note that $\hat{\mathbf{1}}$ and \hat{v}_+ are themselves eigenvectors,

$$\mathbb{T}[\hat{\mathbf{1}}] = \hat{\mathbf{1}}, \quad \mathbb{T}[\hat{v}_+] = [(1-p)e^\kappa + pe^{-\gamma}] \hat{v}_+, \quad (20)$$

so $\hat{Z}_0 \equiv \hat{\mathbf{1}}$, $\lambda_0 \equiv 1$, $\hat{Z}_1 \equiv \hat{v}_+$, and $\lambda_1 \equiv (1-p)e^\kappa + pe^{-\gamma}$. Taking these as base cases, eigenvectors \hat{Z}_n with eigenvalues $\lambda_n = (1-p)e^{n\kappa} + pe^{-n\gamma}$ can be constructed inductively as

$$\hat{Z}_n = (\hat{v}_+)^n + \sum_{k=1}^{\lfloor n/2 \rfloor} \alpha_{n,k} \hat{Z}_{n-2k} = \sum_{k=0}^{\lfloor n/2 \rfloor} \beta_{n,k} (\hat{v}_+)^{n-2k}, \quad (21)$$

where the $\lfloor n/2 \rfloor$ coefficients $\alpha_{n,k}$ or $\beta_{n,k}$ can be found by solving a system of linear equations. This construction is detailed in the Supplement [39].

The operator \hat{Z}_n is controlled when its eigenvalue λ_n is less than one, so that $\langle \hat{Z}_n \rangle \rightarrow 0$ as $t \rightarrow \infty$. From this condition we obtain

$$p_n^* = \frac{e^{n\kappa} - 1}{e^{n\kappa} - e^{-n\gamma}} \quad (22)$$

as the control probability for $\langle \hat{Z}_n \rangle$ to remain finite. When \hat{Z}_n is controlled, all operators of order n are controlled; at $p = p_n^*$ all other eigenvalues of order- n eigenoperators are less than one. For all $n > 0$ we have $p_{n+1}^* > p_n^* > p_c$ and $\lim_{n \rightarrow 0} p_n^* = p_c$, so as p increases above p_c there is a sequence of transitions where operators of increasing order become controllable. This is related to the sequence of moment control rates p_{2n}^{FP} in Eq. (19) obtained from FP: $p_{2n}^* = p_{2n}^{\text{FP}}$ to first order in κ . This confirms that FP captures key features of the exact quantum dynamics in the appropriate limits, and demonstrates that the operators \hat{Z}_n generalize the moment-control picture of the semiclassical analysis to a quantum context.

Quantized Chaotic Map—For an example of control, we look at *quantum* trajectories of Eq. (4) for the Arnold cat map [40]. Despite the complexities brought in by the compactness, several features of the IHO analysis can be extracted, highlighting the universality of our previous analysis. Classically, this map transforms the unit square as

$$\mathbf{r}(t+1) = \begin{pmatrix} 2 & 1 \\ 1 & 1 \end{pmatrix} \mathbf{r}(t) \mod 1. \quad (23)$$

The fixed point is then $\mathbf{r}_0 = 0$ with $\kappa = 2 \ln\left(\frac{1+\sqrt{5}}{2}\right)$. To quantize this system onto N quantum states, we need to introduce an $\hbar = \frac{1}{2\pi N}$ [39] (a consequence of the finite phase space) [41], and the control map in Eq. (4) generalizes with a truncation. This leads to the sharp transition being rounded out into a cross-over, seen in Fig. 3. Inspired by the FP analysis, we track when the *variance* of $\ln(\langle \hat{x}^2 + \hat{p}^2 \rangle)$ over trajectories is maximized to estimate $p_c(\theta)$, which roughly tracks the analytic prediction, see the inset of Fig. 3.

Conclusion—We have shown how to control quantized chaotic maps onto classically unstable fixed points stochastically. This characterizes a whole class of chaotic dynamics, explains the random-walk universality, and

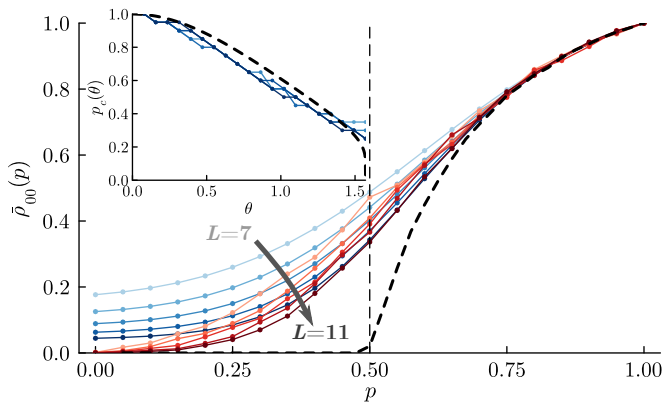


FIG. 3. Comparison of $\bar{\rho}_{00}$ from simulating the quantum cat map (red) and the IHO (blue) for system sizes $L = 7, 8, 9, 10, 11$. There is good agreement in the controlled phase, but the finite and compact phase space of the cat map leads to large differences in the uncontrolled phase. Inset: Estimate for p_c as a function of the control strength θ , c.f. Eq. (4), as the value with maximum variance of $\ln(\langle \hat{x}^2 + \hat{p}^2 \rangle)$. The dashed line shows the analytic form Eq. (1) with $\gamma = -\ln \cos \theta$.

reveals how quantum fluctuations dress the controlled phase. This generalizes previous work [19, 28, 30, 42, 43], which demonstrated how a quantum analog of specific discrete 1D maps can be constructed and exhibit phase transitions to control. It is important to note that the results here are simulable with a classical control map that has quantum-limited noise [39], underscoring the role of quantum fluctuations.

As noted above, this theory cannot access the uncontrolled phase of specific maps. Other quantum phenomena within that phase, such as qubit encoding, interference, and entanglement, can occur and are rich areas for future development. Beyond these, a further question remains of how the *many-body* problem behaves, where the phase space is extensive and Lyapunov exponents can undergo a transition themselves.

Acknowledgments—We thank M. Prasad, A. Chakraborty, T. Iadecola, M. Kulkarni, and J. H. Pixley for discussions and collaboration on related work, and Y. BenTov for discussions on relations to market dynamics. JHW is supported by the NSF CAREER Grant No. DMR-2238895, and SG is supported by NSF CAREER Grant No. DMR-1944967. This work was initiated and performed in part at the Aspen Center for Physics, which is supported by the National Science Foundation Grant No. PHY-1607611. Portions of this research were conducted with high-performance computational resources provided by Louisiana State University (<http://www.hpc.lsu.edu>).

- [1] T. Vicsek, A. Czirók, E. Ben-Jacob, I. Cohen, and O. Shochet, Novel type of phase transition in a system of self-driven particles, *Phys. Rev. Lett.* **75**, 1226 (1995).
- [2] J. Toner and Y. Tu, Long-range order in a two-dimensional dynamical xy model: how birds fly together, *Phys. Rev. Lett.* **75**, 4326 (1995).
- [3] E. Ott, C. Grebogi, and J. A. Yorke, Controlling chaos, *Phys. Rev. Lett.* **64**, 1196 (1990).
- [4] I. Antoniou, V. Basios, and F. Bosco, Probabilistic control of chaos: The β -adic Renyi map under control, *International Journal of Bifurcation and Chaos* **6**, 1563 (1996).
- [5] I. Antoniou, V. Basios, and F. Bosco, Probabilistic Control of Chaos: Chaotic Maps under Control, *Computers & Mathematics with Applications* **34**, 373 (1997).
- [6] I. Antoniou, V. Basios, and F. Bosco, Absolute controllability condition for probabilistic control of chaos, *International Journal of Bifurcation and Chaos* **8**, 409 (1998).
- [7] R. Friedrich and J. Peinke, Description of a Turbulent Cascade by a Fokker-Planck Equation, *Phys. Rev. Lett.* **78**, 863 (1997).
- [8] A. Naert, R. Friedrich, and J. Peinke, Fokker-Planck equation for the energy cascade in turbulence, *Phys. Rev. E* **56**, 6719 (1997).
- [9] R. Benzi, L. Biferale, and F. Toschi, Intermittency in turbulence: Multiplicative random process in space and time, *Journal of Statistical Physics* **113**, 783 (2003).
- [10] J.-B. Durrive, P. Lesaffre, and K. Ferrière, Magnetic fields from multiplicative chaos, *Monthly Notices of the Royal Astronomical Society* **496**, 3015 (2020), <https://academic.oup.com/mnras/article-pdf/496/3/3015/33484791/staa1514.pdf>.
- [11] M. Levy, H. Levy, and S. Solomon, A microscopic model of the stock market : Cycles, booms, and crashes, *Economics Letters* **45**, 103 (1994).
- [12] M. Levy, H. Levy, and S. Solomon, Microscopic Simulation of the Stock Market: the Effect of Microscopic Diversity, *J. Phys. I France* **5**, 1087 (1995).
- [13] M. Levy, S. Solomon, and G. Ram, Dynamical explanation for the emergence of a power law in a stock market model, *International Journal of Modern Physics C* **07**, 65 (1996), <https://doi.org/10.1142/S0129183196000077>.
- [14] U. Frisch and D. D. Sornette, Extreme Deviations and Applications, *J. Phys. I France* **7**, 1155 (1997).
- [15] J. Laherrère and D. Sornette, Stretched exponential distributions in nature and economy: “fat tails” with characteristic scales, *The European Physical Journal B - Condensed Matter and Complex Systems* **2**, 525 (1998).
- [16] H. Takayasu, K. Takayasu, M. Okazaki, K. Marumo, and T. Shimizu, *Paradigms of Complexity: Fractal properties in economics* (World Scientific, Singapore, 2000) pp. 243–258.
- [17] R. Friedrich, J. Peinke, and C. Renner, How to Quantify Deterministic and Random Influences on the Statistics of the Foreign Exchange Market, *Phys. Rev. Lett.* **84**, 5224 (2000).
- [18] D. Sornette, Fokker-Planck equation of distributions of financial returns and power laws, *Physica A: Statistical Mechanics and its Applications* **290**, 211 (2001).
- [19] T. Iadecola, S. Ganeshan, J. H. Pixley, and J. H. Wilson, Measurement and Feedback Driven Entanglement Transition in the Probabilistic Control of Chaos, *Phys. Rev.*

- Lett. **131**, 060403 (2023).
- [20] Y. Herasymenko, I. Gornyi, and Y. Gefen, Measurement-driven navigation in many-body Hilbert space: Active-decision steering, PRX Quantum **4**, 020347 (2023).
 - [21] M. Buchhold, T. Müller, and S. Diehl, Revealing measurement-induced phase transitions by pre-selection (2022), arXiv:2208.10506 [cond-mat.dis-nn].
 - [22] V. Ravindranath, Y. Han, Z.-C. Yang, and X. Chen, Entanglement steering in adaptive circuits with feedback, Phys. Rev. B **108**, L041103 (2023).
 - [23] N. O’Dea, A. Morningstar, S. Gopalakrishnan, and V. Khemani, Entanglement and absorbing-state transitions in interactive quantum dynamics, Phys. Rev. B **109**, L020304 (2024).
 - [24] A. J. Friedman, O. Hart, and R. Nandkishore, Measurement-induced phases of matter require feedback, PRX Quantum **4**, 040309 (2023).
 - [25] L. Piroli, Y. Li, R. Vasseur, and A. Nahum, Triviality of quantum trajectories close to a directed percolation transition, Phys. Rev. B **107**, 224303 (2023).
 - [26] P. Sierant, M. Schirò, M. Lewenstein, and X. Turkeshi, Measurement-induced phase transitions in $(d + 1)$ -dimensional stabilizer circuits, Phys. Rev. B **106**, 214316 (2022).
 - [27] P. Sierant and X. Turkeshi, Controlling Entanglement at Absorbing State Phase Transitions in Random Circuits, Phys. Rev. Lett. **130**, 120402 (2023).
 - [28] C. LeMaire, A. A. Allocca, J. H. Pixley, T. Iadecola, and J. H. Wilson, Separate measurement- and feedback-driven entanglement transitions in the stochastic control of chaos, Phys. Rev. B **110**, 014310 (2024).
 - [29] A. Milekhin and F. K. Popov, Measurement-induced phase transition in teleportation and wormholes, SciPost Phys. **17**, 020 (2024).
 - [30] A. A. Allocca, C. LeMaire, T. Iadecola, and J. H. Wilson, Statistical mechanics of stochastic quantum control: d -adic Rényi circuits, Phys. Rev. E **110**, 024113 (2024).
 - [31] V. Ravindranath, Z.-C. Yang, and X. Chen, Free fermions under adaptive quantum dynamics, Quantum **9**, 1685 (2025).
 - [32] The IHO appears across fields [44–49].
 - [33] M. Prasad, A. Chakraborty, T. Iadecola, M. Kulkarni, J. H. Pixley, S. Ganeshan, and J. H. Wilson, Measurement and feedback-driven adaptive dynamics in the classical and quantum kicked top, *in prep.*
 - [34] A. Serafini, *Quantum Continuous Variables* (CRC Press, London, England, 2021).
 - [35] H. H. Hasegawa and W. C. Saphir, Unitarity and irreversibility in chaotic systems, Phys. Rev. A **46**, 7401 (1992).
 - [36] In classical systems, this operator is ill-defined for Hamiltonian dynamics, requiring the introduction of noise to regularize divergences [39]. In contrast, quantum fluctuations resolve these divergences.
 - [37] D. Sornette and R. Cont, Convergent Multiplicative Processes Repelled from Zero: Power Laws and Truncated Power Laws, J. Phys. I France **7**, 431 (1997).
 - [38] The distribution $\mathcal{Q}_+(\sigma_+)$ is related to the full distribution $\mathcal{Q}(\sigma_+, \sigma_-)$ appearing in Eq. (11) and Eq. (12) by integrating over the allowed values of σ_- , giving a distribution for the values of σ_+ alone.
 - [39] See Supplemental Material for details of the Fokker-Planck analysis, the procedure for constructing eigenvectors of the quantum channel, details of all numerical simulations, and relations to noisy classical control.
 - [40] V. I. Arnold and V. Avez, *Ergodic Problems of Classical Mechanics* (Benjamin, 1968).
 - [41] J. Hannay and M. Berry, Quantization of linear maps on a torus-fresnel diffraction by a periodic grating, Physica D: Nonlinear Phenomena **1**, 267 (1980).
 - [42] H. Pan, S. Ganeshan, T. Iadecola, J. H. Wilson, and J. H. Pixley, Local and nonlocal stochastic control of quantum chaos: Measurement- and control-induced criticality, Phys. Rev. B **110**, 054308 (2024).
 - [43] H. Pan, T. Iadecola, E. M. Stoudenmire, and J. H. Pixley, Control-driven critical fluctuations across quantum trajectories (2025), arXiv:2504.10803 [quant-ph].
 - [44] G. Barton, Quantum mechanics of the inverted oscillator potential, Annals of Physics **166**, 322 (1986).
 - [45] S. Gentilini, M. C. Braidotti, G. Marcucci, E. DelRe, and C. Conti, Physical realization of the Glauber quantum oscillator, Scientific Reports **5**, 15816 (2015).
 - [46] P. Betzios, N. Gaddam, and O. Papadoulaki, The black hole S-Matrix from quantum mechanics, Journal of High Energy Physics **2016**, 131 (2016).
 - [47] S. Dalui, B. R. Majhi, and P. Mishra, Presence of horizon makes particle motion chaotic, Physics Letters B **788**, 486 (2019).
 - [48] S. S. Hegde, V. Subramanyan, B. Bradlyn, and S. Vishveshwara, Quasinormal modes and the hawking-unruh effect in quantum hall systems: Lessons from black hole phenomena, Phys. Rev. Lett. **123**, 156802 (2019).
 - [49] V. Subramanyan, S. S. Hegde, S. Vishveshwara, and B. Bradlyn, Physics of the inverted harmonic oscillator: From the lowest landau level to event horizons, Annals of Physics **435**, 168470 (2021), special issue on Philip W. Anderson.

Fokker-Planck derivation

When the system is initialized in a state such that $\langle \hat{x} \rangle = \langle \hat{p} \rangle = 0$, the late-time value of $\bar{\rho}_{00} = \overline{\langle 0|\rho|0 \rangle}$, which indicates whether the system is controlled, is determined by just a single element of the covariance matrix, $\sigma_+ = \langle (\hat{v}_+)^2 \rangle$. With the known form of the channels \mathbb{S}_κ and \mathbb{C}_γ , the evolution of σ_+ can be expressed as a modified multiplicative process:

$$\sigma_+(t + \delta t) = e^{f(\sigma_+, v)} e^{v \delta t} \sigma_+(t), \quad (\text{A.24})$$

where v is drawn randomly from the distribution

$$\pi(v) = (1 - p) \delta(v - 2\Omega) + p \delta(v + 2\Gamma) \quad (\text{A.25})$$

and

$$f(\sigma_+, v) = \log \left(1 + h_+(v) \frac{e^{-v \delta t} - 1}{2 \sigma_+} \right), \quad (\text{A.26})$$

with $h(2\Omega) = 0$ and $h(-2\Gamma) = 1$; the form of $h(v)$ is not yet determined beyond the values it takes at these two points. The parameters we use for the strength of the quantum channels are $\kappa = \Omega \delta t$ and $\gamma = \Gamma \delta t$. The time step length δt is superfluous in principle; only the strengths of the maps κ and γ are relevant for the dynamics. Including this δt , however, allows us to more easily take a continuous time limit later in the derivation while avoiding pathological behavior of the yet-undetermined function $h(v)$.

Putting $\sigma_+ = \frac{1}{2} e^x$ we can rewrite the dynamics in terms of a modified random walk of the exponential variable x [37]. The factor of $\frac{1}{2}$ is chosen so that the control point $\sigma_+ = \frac{1}{2}$ corresponds to $x = 0$. The time evolution of x is then

$$x(t + \delta t) = T(x(t), v) = x(t) + v \delta t + \tilde{f}(x(t), v), \quad (\text{A.27})$$

where $\tilde{f}(x, v) = f(\frac{1}{2} e^x, v)$. The preimage of $x(t)$ for a given v is

$$T^{-1}(x, v) = x - v \delta t + \tilde{g}(x, v) \quad \text{with} \quad \tilde{g}(x, v) = \log [1 - h(v) (1 - e^{v \delta t}) e^{-x}]. \quad (\text{A.28})$$

Letting $\mathcal{P}(x, t)$ be the distribution of values x takes after many time steps, we have

$$\mathcal{P}(x, t + \delta t) = \int_{-\infty}^{\infty} dv \pi(v) \mathcal{P}(T^{-1}(x, v), t) = \int_{-\infty}^{\infty} dv \pi(v) \mathcal{P}(x - v \delta t + \tilde{g}(x, v), t) \quad (\text{A.29})$$

$$= \int_{-\infty}^{\infty} d(\delta v) \pi(\bar{v} + \delta v) \mathcal{P}(x - \bar{v} \delta t - \delta v \delta t + \tilde{g}(x, \bar{v} + \delta v), t) \quad (\text{A.30})$$

$$\approx \mathcal{P}(T^{-1}(x, \bar{v}), t) + \delta t^2 \frac{\langle \delta v^2 \rangle}{2} \left[\frac{1}{\delta t^2} \frac{\partial^2 \tilde{g}(x, v)}{\partial v^2} \Big|_{v=\bar{v}} \frac{\partial \mathcal{P}(y, t)}{\partial y} + \left(1 - \frac{1}{\delta t} \frac{\partial \tilde{g}(x, v)}{\partial v} \Big|_{v=\bar{v}} \right)^2 \frac{\partial^2 \mathcal{P}(y, t)}{\partial y^2} \right]_{y=T^{-1}(x, \bar{v})}, \quad (\text{A.31})$$

where in the second line we put $v = \bar{v} + \delta v$ with $\bar{v} = \int dv v \pi(v) = 2\Omega - 2p(\Gamma + \Omega)$ the average value of v , so that $\int dv \delta v \pi(v) = 0$. In the final line we expand in δv , which involves expanding both the distribution \mathcal{P} and the function \tilde{g} . This assumes that $\pi(v)$ is relatively sharply peaked around \bar{v} . We also pull a factor of δt^2 from the entire bracketed expression. Using one of these factors of δt , the expectation value of δv^2 can be manipulated to give a diffusion constant,

$$\mathcal{D} \equiv \delta t \frac{\langle \delta v^2 \rangle}{2} = \frac{\delta t}{2} \int_{-\infty}^{\infty} dv \pi(v) (v - \bar{v})^2 \quad (\text{A.32})$$

$$= \frac{\delta t}{2} [4p^2(1 - p)(\Gamma + \Omega)^2 + 4p(1 - p)^2(\Gamma + \Omega)^2] = 2p(1 - p)(\Gamma + \Omega)^2 \delta t. \quad (\text{A.33})$$

If we define a step size $\ell = v \delta t$ then we see that the diffusion constant is the mean-square step size per time step. It grows with the difference between the two possible values of v —if they are very different, then trajectories will diverge quickly, i.e. fast diffusion.

Now consider a limit such that our dynamics are well-approximated as continuous in time. We can accomplish this by considering δt small with fixed Ω, Γ , but we should think of this as the limit of weak maps, i.e. small κ, γ .

Expanding in δt helps us avoid issues with the yet-undetermined function $h(v)$, but in the end the value of δt is set to 1.

Returning to Eq. (A.31), we bring $P(T^{-1}(x, \bar{v}), t)$ to the left-hand side and divide both sides by δt giving

$$\frac{1}{\delta t} [\mathcal{P}(x, t + \delta t) - \mathcal{P}(T^{-1}(x, \bar{v}), t)] \xrightarrow{\delta t \text{ small}} \frac{\partial \mathcal{P}(x, t)}{\partial t} + \bar{v} (1 - h(\bar{v})e^{-x}) \frac{\partial \mathcal{P}(x, t)}{\partial x}, \quad (\text{A.34})$$

on the left-hand side, where we have expanded $T^{-1}(x, \bar{v}) = x - \bar{v} \delta t + \tilde{g}(x, \bar{v})$ using $\tilde{g}(x, v) \approx \delta t v h(v) e^{-x} + \delta t^2 \frac{v^2}{2} (1 - h(v)e^{-x})h(v)e^{-x}$. This could alternatively be written as a total time derivative with $x(t)$ evolving ballistically with velocity \bar{v} .

The right-hand side of Eq. (A.31) has factors related to the derivatives of $\tilde{g}(x, v)$,

$$\frac{1}{\delta t} \frac{\partial \tilde{g}(x, v)}{\partial v} \Big|_{v=\bar{v}} = \frac{\partial (v h(v))}{\partial v} \Big|_{v=\bar{v}} e^{-x} + O(\delta t) \quad (\text{A.35})$$

$$\frac{1}{\delta t^2} \frac{\partial^2 \tilde{g}(x, v)}{\partial v^2} \Big|_{v=\bar{v}} = \frac{1}{\delta t} \frac{\partial^2 (v h(v))}{\partial v^2} \Big|_{v=\bar{v}} e^{-x} + \frac{1}{2} \frac{\partial^2 [v^2 (1 - h(v)e^{-x})h(v)]}{\partial v^2} \Big|_{v=\bar{v}} e^{-x} + O(\delta t). \quad (\text{A.36})$$

The $1/\delta t$ in the first term of Eq. (A.36) presents a problem. Though we need to expand the derivatives of \mathcal{P} in powers of δt since they are evaluated at $T^{-1}(x, \bar{v})$ and not x , when the $1/\delta t$ term of Eq. (A.36) multiplies $\partial \mathcal{P}(x, t)/\partial x$ there is no factor of δt to cancel it, leading to a divergence for small δt unless we impose a condition to cancel it in general,

$$\frac{\partial^2 (v h(v))}{\partial v^2} = 0 \quad \Rightarrow \quad h(v) = \frac{\Gamma v - 2\Omega}{v \Gamma + \Omega}. \quad (\text{A.37})$$

Since $h(v)$ was not determined when introduced besides its value at $v = 2\Omega$ and $v = -2\Gamma$ we are free to use this form to satisfy this additional constraint and ensure a well-formed Fokker-Planck equation in the continuous time limit. As a result of this condition, no additional terms involving additional derivatives of P will appear. The needed derivatives of \tilde{g} are

$$\frac{\partial (v h(v))}{\partial v} \Big|_{v=\bar{v}} = \frac{\Gamma}{\Gamma + \Omega} = \frac{\gamma}{\kappa + \gamma} = 1 - p_c \equiv \lambda \quad (\text{A.38})$$

$$\begin{aligned} \frac{1}{2} \frac{\partial^2 [v^2 (1 - h(v)e^{-x})h(v)]}{\partial v^2} \Big|_{v=\bar{v}} e^{-x} \\ = \left(1 - \frac{\Gamma}{\Gamma + \Omega} e^{-x}\right) \frac{\Gamma}{\Gamma + \Omega} e^{-x} = (1 - \lambda e^{-x}) \lambda e^{-x} \end{aligned} \quad (\text{A.39})$$

We therefore have the Fokker-Planck equation

$$\frac{\partial \mathcal{P}(x, t)}{\partial t} = -v(x) \frac{\partial \mathcal{P}(x, t)}{\partial x} + \mathcal{D} r(x) \frac{\partial}{\partial x} \left[r(x) \frac{\partial \mathcal{P}(x, t)}{\partial x} \right], \quad (\text{A.40})$$

with

$$r(x) = 1 - \lambda e^{-x} \quad (\text{A.41})$$

$$v(x) = \bar{v} (1 - h(\bar{v})e^{-x}) = \left(\bar{v} + 2\kappa \frac{\lambda}{e^x - \lambda} \right) r(x). \quad (\text{A.42})$$

Notice that everywhere we have a spatial derivative we have a factor of $r(x)$, suggesting that we can change coordinates to make Eq. (A.40) take a cleaner form. Putting

$$z \equiv \log(e^x - \lambda) \Rightarrow \frac{\partial}{\partial z} = r(x) \frac{\partial}{\partial x}, \quad (\text{A.43})$$

and defining $P(z, t) = \mathcal{P}(x(z), t)$ we obtain

$$\frac{\partial P(z, t)}{\partial t} = -(\bar{v} + 2\gamma p_c e^{-z}) \frac{\partial P(z, t)}{\partial z} + \mathcal{D} \frac{\partial^2 P(z, t)}{\partial z^2} \quad (\text{A.44})$$

$$= -2\gamma p_c e^{-z} P(z, t) - \frac{\partial [(\bar{v} + 2\gamma p_c e^{-z}) P(z, t)]}{\partial z} + \mathcal{D} \frac{\partial^2 P(z, t)}{\partial z^2}. \quad (\text{A.45})$$

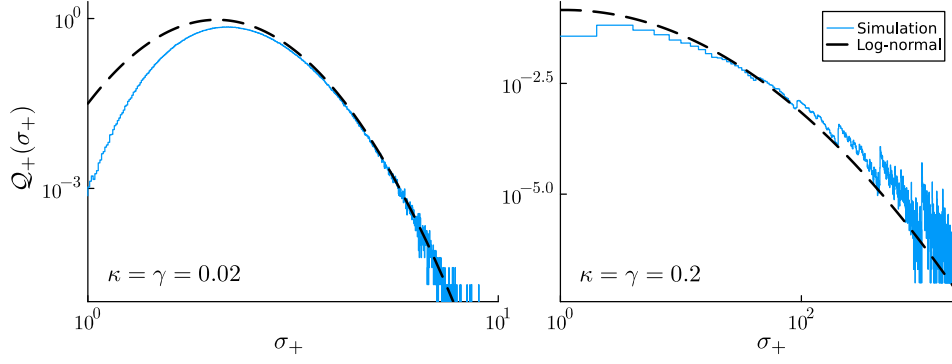


FIG. 4. The early-time distribution of values taken by σ_+ in numerical simulations compared to the predicted log-normal form of $\mathcal{Q}_\sigma(\sigma_+)$, shown in a log-log plot. The simulations average over 5×10^6 stochastic trajectories for two parameter regimes.

As a result, the original element of the covariance matrix is $\sigma_+ = \frac{1}{2}e^x = \frac{1}{2}(e^z - p_c + 1)$, with the control point $\sigma_+ = \frac{1}{2}$ now equating to $z = \log(p_c)$.

The Fokker-Planck equation obtained here has followed from the exact stochastic dynamics on σ_+ , and we see that the equation analyzed in the main text,

$$\frac{\partial P(z, t)}{\partial t} = -\bar{v} \frac{\partial P(z, t)}{\partial z} + \mathcal{D} \frac{\partial^2 P(z, t)}{\partial z^2}, \quad (\text{A.46})$$

along with constraint $z > -\ln(2)$, agrees with this exact equation in the large- z limit. Accordingly, the solutions for the distribution $P(z, t)$ and therefore $\mathcal{Q}_+(\sigma_+)$ far from this boundary are also valid, power-law at $p = p_c$ and log-normal for early times and $p \neq p_c$. The power-law critical behavior is discussed in the main text, and in Fig. 4 we also show agreement with the log-normal distribution in the appropriate limits.

Eigenvectors of the Stochastic Evolution

The stochastic dynamics we consider generates time evolution in the Heisenberg picture as

$$\mathbb{T}[\hat{\mathcal{O}}(t+1)] = (1-p)\mathbb{S}_\kappa[\hat{\mathcal{O}}(t)] + p\mathbb{C}_\gamma[\hat{\mathcal{O}}(t)], \quad (\text{A.47})$$

where $\hat{\mathcal{O}}$ is a generic operator, and \mathbb{S}_κ and \mathbb{C}_γ are the squeezing and control channels. While all the eigenvectors of the individual channels \mathbb{S}_κ and \mathbb{C}_γ are simple to calculate, eigenvectors for the full channel \mathbb{T} are not as straightforward to obtain. Here we now construct an infinite set these eigenvectors that will allow us to draw important conclusions about the controlled phase of this model.

We first note the useful identities

$$(\hat{v}_+)^k = \sum_{l=0}^{\lfloor k/2 \rfloor} \underbrace{\frac{(2l-1)!!}{2^l} \binom{k}{2l}}_{\equiv \mathcal{A}_{k, k-2l}} : (\hat{v}_+)^{k-2l} : = : (\hat{v}_+)^k : + \sum_{l=1}^{\lfloor k/2 \rfloor} \mathcal{A}_{k, k-2l} : (\hat{v}_+)^{k-2l} : \quad (\text{A.48})$$

$$: (\hat{v}_+)^k : = \sum_{l=0}^{\lfloor k/2 \rfloor} \underbrace{(-1)^l \frac{(2l-1)!!}{2^l} \binom{k}{2l}}_{\equiv (\mathcal{A}^{-1})_{k, k-2l}} (\hat{v}_+)^{k-2l}, \quad (\text{A.49})$$

allowing us to transform between $(\hat{v}_+)^k$ and $: (\hat{v}_+)^k :$, where

$$: (\hat{v}_+)^k : = \left(\frac{e^{-i\pi/4}}{\sqrt{2}} \right)^k \sum_{j=0}^k \binom{k}{j} (i\hat{a}^\dagger)^j \hat{a}^{k-j} \quad (\text{A.50})$$

has normally-ordered ladder operators, so that

$$\mathbb{C}_\gamma[: (\hat{v}_+)^k :] = e^{-k\gamma} : (\hat{v}_+)^k :. \quad (\text{A.51})$$

Eq. (A.48) is simple to derive, and we obtain Eq. (A.49) by noting that $\mathcal{A}_{k,k'}$ are the components of a triangular matrix—we have only nonzero elements for $k > k'$. The properties of triangular matrices then allow direct computation of \mathcal{A}^{-1} .

Two low-order eigenvectors of \mathbb{T} are straightforward:

$$\mathbb{S}_\kappa[\hat{1}] = \mathbb{C}_\gamma[\hat{1}] = \hat{1} \quad \Rightarrow \quad \mathbb{T}[\hat{1}] = \hat{1} \quad (\text{A.52})$$

$$\mathbb{S}_\kappa[\hat{v}_+] = e^\kappa \hat{v}_+, \quad \mathbb{C}_\gamma[\hat{v}_+] = e^{-\gamma} \hat{v}_+ \quad \Rightarrow \quad \mathbb{T}[\hat{v}_+] = [(1-p)e^\kappa + p e^{-\gamma}] \hat{v}_+. \quad (\text{A.53})$$

so we can define the corresponding eigenvalues $\lambda_0 = 1$ and $\lambda_1(p) = (1-p)e^\kappa + p e^{-\gamma}$. We now build eigenvectors of \mathbb{T} inductively using these as base cases.

Assume that for some fixed n we have a set of operators $\{\hat{Z}_k\}$ for $k = 0, 2, \dots, n-2$ (n even) or $k = 1, 3, \dots, n-2$ (n odd), with $\hat{Z}_0 \equiv \hat{1}$, $\hat{Z}_1 \equiv \hat{v}_+$, and

$$\mathbb{T}[\hat{Z}_k] = \lambda_k(p) \hat{Z}_k, \quad (\text{A.54})$$

with known eigenvalues $\lambda_k(p)$. Additionally, assume that we know how to write any of these \hat{Z}_k as a sum over the operators in this set with smaller index as

$$\hat{Z}_k = (\hat{v}_+)^k + \sum_{l=1}^{\lfloor k/2 \rfloor} \alpha_{k,k-2l} \hat{Z}_{k-2l} = \sum_{l=0}^{\lfloor k/2 \rfloor} \beta_{k,k-2l} (\hat{v}_+)^{k-2l}, \quad (\text{A.55})$$

where all coefficients $\alpha_{k,k-2l}$ are known and the coefficients $\beta_{k,k-2l}$ can be written in terms of the α s by expanding all \hat{Z}_{k-2l} in this same way and collecting powers of \hat{v}_+ —the first few are $\beta_{k,k} = 1$, $\beta_{k,k-2} = \alpha_{k,k-2}$, and $\beta_{k,k-4} = \alpha_{k,k-4} + \alpha_{k,k-2}\alpha_{k-2,k-4}$. For $n = 2$ or 3 the set of known operators is simply $\hat{Z}_0 = \hat{1}$ or $\hat{Z}_1 = \hat{v}_+$ alone, and these expansions are trivial.

Now write a new operator,

$$\hat{Z}_n = (\hat{v}_+)^n + \sum_{k=1}^{\lfloor n/2 \rfloor} \alpha_{n,n-2k} \hat{Z}_{n-2k} \quad (\text{A.56})$$

$$= (\hat{v}_+)^n + \sum_{k=1}^{\lfloor n/2 \rfloor} \beta_{n,n-2k} (\hat{v}_+)^{n-2k} \quad (\text{A.57})$$

where $\alpha_{n,n-2k}$ are $\lfloor n/2 \rfloor$ undetermined constants, one for each k , and $\beta_{n,n-2k}$ can be written in terms of these α s as in Eq. (A.55). This new operator evolves under \mathbb{T} as

$$\begin{aligned} \mathbb{T}[\hat{Z}_n] &= \mathbb{T}[(\hat{v}_+)^n] + \sum_{k=1}^{\lfloor n/2 \rfloor} \alpha_{n,n-2k} \mathbb{T}[\hat{Z}_{n-2k}] \\ &= (1-p)\mathbb{S}_\kappa[(\hat{v}_+)^n] + p \sum_{k=0}^{\lfloor n/2 \rfloor} \mathcal{A}_{n,n-2k} \mathbb{C}_\gamma [: (\hat{v}_+)^{n-2k} :] + \sum_{k=1}^{\lfloor n/2 \rfloor} \alpha_{n,n-2k} \lambda_{n-2k}(p) \hat{Z}_{n-2k} \\ &= (1-p)e^{n\kappa} (\hat{v}_+)^n + p \underbrace{\sum_{k=0}^{\lfloor n/2 \rfloor} \mathcal{A}_{n,n-2k} e^{-(n-2k)\gamma} : (\hat{v}_+)^{n-2k} :}_{\text{separate out } k=0 \text{ term, noting } \mathcal{A}_{n,n}=1} + \sum_{k=1}^{\lfloor n/2 \rfloor} \alpha_{n,n-2k} \lambda_{n-2k}(p) \hat{Z}_{n-2k} \\ &= (1-p)e^{n\kappa} (\hat{v}_+)^n + p e^{-n\gamma} \underbrace{: (\hat{v}_+)^n :}_{\text{use Eq. (A.48)}} + p \sum_{k=1}^{\lfloor n/2 \rfloor} \mathcal{A}_{n,n-2k} e^{-(n-2k)\gamma} : (\hat{v}_+)^{n-2k} : + \sum_{k=1}^{\lfloor n/2 \rfloor} \alpha_{n,n-2k} \lambda_{n-2k}(p) \hat{Z}_{n-2k} \\ &= \underbrace{[(1-p)e^{n\kappa} + p e^{-n\gamma}]}_{\equiv \lambda_n(p)} (\hat{v}_+)^n + p \sum_{k=1}^{\lfloor n/2 \rfloor} \mathcal{A}_{n,n-2k} \left[e^{-(n-2k)\gamma} - e^{-n\gamma} \right] : (\hat{v}_+)^{n-2k} : + \sum_{k=1}^{\lfloor n/2 \rfloor} \alpha_{n,n-2k} \lambda_{n-2k}(p) \hat{Z}_{n-2k} \\ &= \lambda_n(p) \hat{Z}_n + \sum_{k=1}^{\lfloor n/2 \rfloor} \left\{ p \mathcal{A}_{n,n-2k} \left[e^{-(n-2k)\gamma} - e^{-n\gamma} \right] : (\hat{v}_+)^{n-2k} : + \alpha_{n,n-2k} [\lambda_{n-2k}(p) - \lambda_n(p)] \hat{Z}_{n-2k} \right\} \end{aligned}$$

We now use Eq. (A.49) and Eq. (A.55) to express all operators in the expression in brackets as powers of \hat{v}_+ , and re-indexing and reordering the sums gives

$$\mathbb{T}[\hat{Z}_n] = \lambda_n(p)\hat{Z}_n + \sum_{l=1}^{\lfloor n/2 \rfloor} \sum_{k=1}^l \left\{ p \left[e^{-(n-2k)\gamma} - e^{-n\gamma} \right] \mathcal{A}_{n,n-2k}(\mathcal{A}^{-1})_{n-2k,n-2l} \right. \\ \left. + [\lambda_{n-2k}(p) - \lambda_n(p)] \alpha_{n,n-2k} \beta_{n-2k,n-2l} \right\} (\hat{v}_+)^{n-2l} \quad (\text{A.58})$$

$$\equiv \lambda_n(p)\hat{Z}_n + \sum_{k=1}^{\lfloor n/2 \rfloor} \mathcal{C}_{n,n-2k} (\hat{v}_+)^{n-2k}. \quad (\text{A.59})$$

Demanding that all of the $\lfloor n/2 \rfloor$ coefficients $\mathcal{C}_{n,n-2k}$ vanish enforces particular values for the unknowns $\alpha_{n,n-2k}$. This demand can always be satisfied because \mathcal{C} can be expressed as a triangular matrix multiplying a vector of powers of \hat{v}_+ . For $k=1$, $\mathcal{C}_{n,n-2} = 0$ gives an equation that contains only a single unknown, $\alpha_{n,n-2}$, and we find

$$\alpha_{n,n-2} = \frac{p \left[e^{-(n-2)\gamma} - e^{-n\gamma} \right] \mathcal{A}_{n,n-2}(\mathcal{A}^{-1})_{n-2,n-2}}{[\lambda_{n-2}(p) - \lambda_n(p)] \beta_{n-2,n-2}}, \quad (\text{A.60})$$

entirely in terms of known quantities. For $k=2$, $\mathcal{C}_{n,n-4} = 0$ gives an equation that depends on $\alpha_{n,n-4}$ and the now determined $\alpha_{n,n-2}$, allowing for the former to be obtained explicitly. The pattern continues, allowing us to solve for all $\alpha_{n,n-2k}$ in sequence.

In the end we are left with

$$\mathbb{T}[\hat{Z}_n] = \lambda_n(p)\hat{Z}_n \quad (\text{A.61})$$

so this posited operator is a new eigenvector of \mathbb{T} with eigenvalue $\lambda_n(p) = (1-p)e^{n\kappa} + pe^{-n\gamma}$. We can repeat this process *ad infinitum* to construct an infinite tower of eigenvectors and eigenvalues for all integers n . This also confirms the consistency of the assumed form of the operators \hat{Z}_k in Eq. (A.55). We can also rewrite Eq. (A.56) as

$$(\hat{v}_+)^n = \hat{Z}_n - \sum_{k=1}^{\lfloor n/2 \rfloor} \alpha_{n,n-2k} \hat{Z}_{n-2k}, \quad (\text{A.62})$$

giving a way to express any power of \hat{v}_+ in terms of eigenvectors $\{\hat{Z}_k\}$.

Operator evolution and critical points

Though the set $\{\hat{Z}_n\}$ does not comprise a complete set of eigenvectors of \mathbb{T} , it allows us to examine the controllability of generic operators. With repeated application of \mathbb{T} , the operators \hat{Z}_k acquire factors of the corresponding $\lambda_n(p)$, and will diverge whenever $\lambda_n(p) > 1$, allowing us to define a critical control rate for each n as

$$\lambda_n(p_n^*) = 1 \quad \Rightarrow \quad p_n^* = \frac{e^{n\kappa} - 1}{e^{n\kappa} - e^{-n\gamma}}, \quad (\text{A.63})$$

with divergence occurring for $p < p_n^*$ as $t \rightarrow \infty$. For any $\kappa, \gamma > 0$ we have $p_{n+1}^* > p_n^*$, so that operators of higher order require more frequent interventions to control. A generic operator $\hat{\mathcal{O}}$ containing terms up to n th order in canonical operators can be expanded in terms of the eigenvectors of \mathbb{T} . This expansion will generically contain \hat{Z}_k terms for all $k \leq n$, and so will diverge at late times for all $p < p_n^*$.

Stochastic Control of the Cat Map

Using Berry's method of quantizing linear maps [41], we generate a quantum version of Arnold's cat map [40], which is a well known chaotic map. The classical cat map is defined to act on a two-dimensional parameter space as

$$\begin{pmatrix} x' \\ y' \end{pmatrix} = \begin{pmatrix} 2 & 1 \\ 1 & 1 \end{pmatrix} \begin{pmatrix} x \\ y \end{pmatrix} \mod 1. \quad (\text{A.64})$$

The quantized cat map propagator acts on states $|Q\rangle$ for $Q = 0, \dots, N-1$ (and $x = Q/N$ is the point in the phase space) is given by:

$$\langle Q_1|U|Q_2\rangle = \sqrt{\frac{i}{N}} \exp\left(\frac{i\pi}{N}(Q_1^2 + (Q_2 - Q_1)^2)\right) \quad (\text{A.65})$$

where N must be a positive even integer. We can map this to phase space $|Q\rangle = \frac{1}{N} \sum_P e^{2\pi i Q P/N} |P\rangle$, where now $P = 0, \dots, N-1$, and if we want to impose $y = P/N$, this necessarily means $e^{2\pi i Q P/N} \rightarrow e^{2\pi N i x y} = e^{i x y / \hbar}$, which works if we let

$$\hbar = \frac{1}{2\pi N}.$$

Therefore, finite-size in these compact discrete maps is intimately tied to its classicality.

The classical cat map has an unstable fixed point at the origin $(0,0)$, and we want to control the system onto this point. Near the fixed point, the cat map dynamics can be approximated by an inverted harmonic oscillator, and we can derive exactly how by finding the eigenvalues and eigenvectors of the map in Eq. (A.64) in terms of $\varphi = \frac{1+\sqrt{5}}{2}$, for which we have $\{\varphi^2, \varphi^{-2}\}$ as the eigenvalues and $\{(\varphi, 1)^T, (-\varphi^{-1}, 1)^T\}$ as the (unnormalized) eigenvectors. This model, therefore has $\kappa = 2 \ln \varphi$, and to get to the number basis, we consider the basis that diagonalizes

$$\tilde{H} = 2 - \cos(\hat{x}) - \cos(\hat{p}), \quad \tilde{H} |n\rangle = E_n |n\rangle,$$

for $\hat{x} |Q\rangle = Q/N |Q\rangle$ and $\hat{p} |P\rangle = P/N |P\rangle$. In this basis, we define the raising and lower operators $a |n\rangle = \sqrt{n} |n-1\rangle$ and $a^\dagger |n\rangle = \sqrt{n+1} |n+1\rangle$ and use these to build the Kraus operators from the main text. The Kraus operators need no modification except to be truncated to a smaller space $n = 0, \dots, N-1$.

The quantum simulations are then done on *trajectories* to maintain state purity and avoid simulating full density matrices. Therefore, when control is done, we choose which Kraus operator K_m to apply based on its Born probability

$$P_m^{\text{Born}} = \langle \psi | \hat{K}_m^\dagger \hat{K}_m | \psi \rangle. \quad (\text{A.66})$$

where, $|\psi\rangle$ is the system wavefunction and $0 \leq m \leq N-1$.

We choose p to be the measurement rate, and perform the unitary cat map evolution at a rate of $1-p$. Performing this stochastic evolution, we can average over trajectories to obtain quantities like the order parameter $\bar{\rho}_{00}(t) = \overline{|\langle 0 | \psi_t \rangle|^2}$, where (\dots) represents averaging over trajectories.

There are large finite-size effects in this quantity, see Fig. 5(left), and inspired by the Fokker-Planck analysis, we find that $\text{var}(\log \langle \psi_t | \hat{n} + 1/2 | \psi_t \rangle)$ (the variance of the log over trajectories) has a maximum near the analytic prediction for the transition, see Fig. 5(right).

Classical noise in the control map

We can simulate similar features to the full quantum problem but with classical probability distributions using an Ornstein-Uhlenbeck process in phase space: x evolves as

$$\frac{dx}{dt} = -\gamma x + \sqrt{2D} \xi(t), \quad (\text{A.67})$$

where $\langle \xi(t) \xi(s) \rangle = \delta(t-s)$, and similarly for p . The Fokker-Planck equation for the distribution of values of x (or p) is well known

$$\frac{\partial P}{\partial t} = \gamma \frac{\partial}{\partial x} (xP) + D \frac{\partial^2 P}{\partial x^2}, \quad (\text{A.68})$$

so the distribution evolves with the kernel

$$K(x, t; x', t') = \sqrt{\frac{\gamma}{2\pi D(1 - e^{-2\gamma(t-t')})}} \exp \left[-\frac{\gamma}{2D} \frac{(x - x' e^{-\gamma(t-t')})^2}{1 - e^{-2\gamma(t-t')}} \right]. \quad (\text{A.69})$$

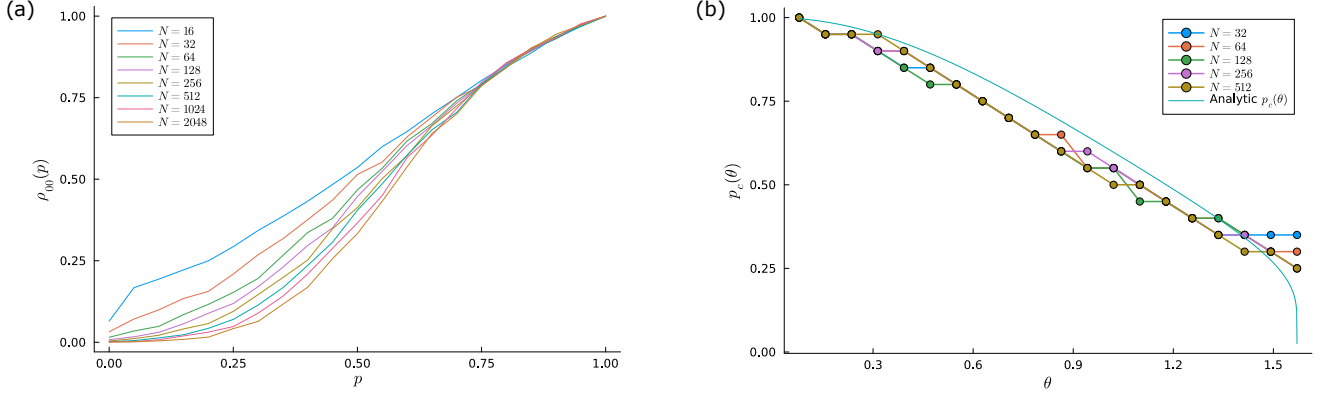


FIG. 5. (a) $\bar{\rho}_{00}$ as a function of p obtained as the trajectory average of simulating the cat map with stochastic control for a range of system sizes. (b) Estimate for the value of p_c as a function of the control strength θ , extracted as the value that maximizes the variance of $\ln(\langle \hat{x}^2 + \hat{p}^2 \rangle)$.

Taking an initial Gaussian distribution, $P(x, 0) = \frac{1}{\sqrt{2\pi}\sigma} e^{-\frac{(x-x_0)^2}{2\sigma^2}}$, convolution with the evolution kernel yields another Gaussian

$$P(x, t) = \frac{1}{\sqrt{2\pi(\sigma e^{-2\gamma t} + \frac{D}{\gamma}(1 - e^{-2\gamma t}))}} \exp \left[-\frac{1}{2} \frac{(x - x_0 e^{-\gamma t})^2}{\sigma e^{-2\gamma t} + \frac{D}{\gamma}(1 - e^{-2\gamma t})} \right] \quad (\text{A.70})$$

Therefore we can track how control changes Gaussian probability distributions

$$\begin{aligned} x &\mapsto e^{-\gamma t} x \\ \sigma &\mapsto e^{-2\gamma t} \sigma + \frac{D}{\gamma} (1 - e^{-2\gamma t}) \end{aligned} \quad (\text{A.71})$$

This will be true for both x and p (or any other basis). We also have a chaotic map which behaves the same as indicated in the main text. This is the same as what we have for Gaussian bosonic states.

Interleaving chaos and control stochastically, we can build up a distribution of v_{\pm} and σ_{\pm} . The controlled “distribution” then takes the form

$$P_0(x, p) = \frac{1}{2\pi D/\gamma} \exp \left[-\frac{\gamma}{2D} (x^2 + p^2) \right]. \quad (\text{A.72})$$

This form can now be integrated against another Gaussian

$$P(v_+, v_-) = \frac{1}{2\pi \sqrt{\sigma_+ \sigma_-}} e^{-\frac{v_+^2}{2\sigma_+} - \frac{v_-^2}{2\sigma_-}}, \quad (\text{A.73})$$

to give

$$\frac{4\pi D}{\gamma} \int dv_- dv_+ P(v_+, v_-) P_0(v_+, v_-) = \frac{2D/\gamma}{\sqrt{(D/\gamma + \sigma_+)(D/\gamma + \sigma_-)}}. \quad (\text{A.74})$$

The last step is to note that we average over trajectories so there is a *probability distribution* of σ_{\pm} which we call $\mathbb{Q}(\sigma_+, \sigma_-)$. For this, we can compute the true probability distribution

$$P_{\text{full}}(x_+, x_-) = \int d\sigma_+ d\sigma_- \mathbb{Q}(\sigma_+, \sigma_-) P(x_+, x_-), \quad (\text{A.75})$$

and we therefore have the final expression to find the overlap with the noisy controlled distribution

$$\frac{4\pi D}{\gamma} \int dx_- dx_+ P_{\text{full}}(x_+, x_-) P_0(x_+, x_-) = \int d\sigma_+ d\sigma_- \frac{(2D/\gamma) \mathbb{Q}(\sigma_+, \sigma_-)}{\sqrt{(D/\gamma + \sigma_+)(D/\gamma + \sigma_-)}}, \quad (\text{A.76})$$

If we have quantum-limited noise if $D/\gamma = \frac{1}{2}$. This shows that the quantum case is related to a noisy classical problem with a particular form of noise.